Communications in Physics, Vol. 31, No. 3 (2021), pp. 335-342
DOI:https://doi.org/10.15625/0868-3166/2021/16029

CREATION OF HOLLOW-GAUSSIAN BEAM FOR OPTICAL TRAP BY DUAL-BEAM NONLIEAR FABRY-PEROT INTERFEROMETER

NGUYEN MANH THANG[1,†] AND HO QUANG QUY[2]

[1]*Academy of Military Science and Technology, 17, Hoang Sam, Cau Giay, Ha Noi.*
[2]*Ho Chi Minh University of Food Industry, 140, Le Trong Tan, Tan Phu, HCM City*

E-mail: [†]thangnm@jmst.info

Received 23 April 2021
Accepted for publication 25 May 2021
Published 4 July 2021

Abstract. *In this paper, a model of dual-beam nonlinear Fabry-Perot interferometer (DBNFPI) for creation laser hollow-Gaussian beam (HGB) is investigated. It includes a thin film of organic dye sandwiched between two optical mirrors, and irradiated by two signal and pump laser Gaussian beams. Based on the equation describing the output-input relation of intensities concerning pump intensity and the expression of the spatial intensity distribution of output signal beam (OSB), the range of pump intensity and collection of designed parameters are numerically calculated and discussed for HGB creation. These results give us the opportunity to use DBNFPI for optical trap of low-index dielectric particles.*

Keywords: nonlinear optics; optical bistable device; laser gaussian beam;
laser hollow-gaussian beam.

Classification numbers: 42.65.-k; 07.60.-j.

I. INTRODUCTION

The high-index particle which has reflective index higher than that of embedding fluid can be trapped using the highly focused laser beam. The intensity spatial Gaussian distribution of this laser beam is the main fact to trap dielectric high-index particle. Otherwise, the low-index particle which has reflective index lower than that of embedding fluid will be trapped by the laser hollow-Gaussian, only [1]. Principally, the conventional laser beam generated directly from resonator always has its Gaussian shape, but not hollow-Gaussian one. The hollow-Gaussian beams (HGB) are expected to be useful for particle trapping, free-space optical communication [2], optical limiting, low power all-optical devices [3].There is a lot of ways to create the HGB [4–10].

©2021 Vietnam Academy of Science and Technology

It could begenerated by the effective thermal focal length at steady state [3, 11], by beam shaping with phase-only liquid crystal spatial light modulator [5], through nonlinear interaction of photons with orbital angular momentum [12], by thermal lens effect [3] as well as in strongly nonlocal nonlinear media [7]. The main fact plays the role of the creation of HGB is the spatial phase modulation of light propagating through the nonlinear medium [5,8,10]. However, the hollow width of created hollow-Gaussian beam is not controllable till now. Principally, the bistable optical device operates based on the optical phase modulation in Kerr medium [13–24]. In the last work [25] we investigated the bistability of nonlinear Fabry-Perot interferometer (NFPI) sandwiched oil red O (ORO) with a very thin thickness of 0.1 mm. The input-output relation of intensities, the peak flattening of the Gaussian beam are presented. The optical bistable properties of NFPI depending on the input power is observed. However, these properties were only considered in the case of the laser beam irradiated on an ideal point. There is a question what will happens when the input beam is Gaussian, and the spatial phase modulation is controlled by another Gaussian one. We predict that the output beam will be reshaped to different GB shapes, one of them is HGB.

In this paper we present a proposed model of DBNFPI. The equation describing the output-input relation of signal light intensities concerning the pump intensity and the expression of intensity distribution of OSB with different shapes are derived. The range of the pump intensity suitable to design parameters to create HGB is numerically calculated. Finally, we discuss the capability to use DBNFPI for optical trap low-index particles.

II. MODEL FOR SIMULATION

The design model of proposed DBNFPI is illustrated in Fig. 1. A nonlinear medium (NM) is the thin film of ORO with thickness$d$, nonlinear refractive coefficientn_2 sandwiched between two optical mirrors to make NFPI. The input mirror has reflection coefficients $R(\lambda_s) = R\%$and $R(\lambda_p) = 0\%$, the output one has reflection coefficients $R(\lambda_s) = R\%$and $R(\lambda_p) = 100\%$. The signal and pump beams of wavelengthsλ_s andλ_p, respectively are propagated perpendicular to the input mirror of NFPI by a dichroic mirror, then focused into Gaussian beam (GB) of waist $W_0$by a telescope with lenses L_1 and L_2.

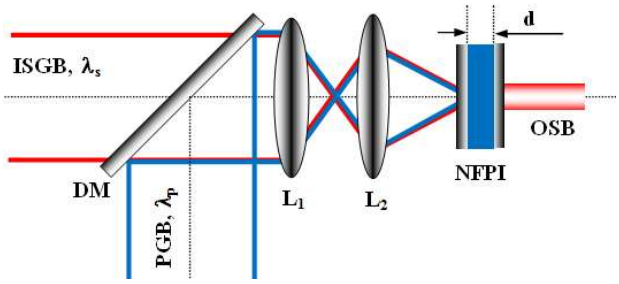

Fig. 1. Principal model of DBNFPI. ISGB: Input signal Gaussian beam, OSB: Output signal beam, PGB: pump Gaussian beam, DM: dichroic mirror, NFPI: Nonlinear Fabry-Perot interferometer with ORO, L_1, L_2: Lenses.

With chosen reflection coefficients, the pump light plays the role in nonlinear effect (Kerr effect) to modulate reflective index of NM inside NFPI, only. At the same time, the signal light plays both roles in nonlinear and feedback effects. Thus, the interference and phase modulation inside NFPI occur for the signal light, only. The electric field of input signal light $E_{in,s}$ and pump

light E_{pump} can be simplified as follows:

$$E_{in,s} = A_{0,s} exp[i(\omega_s t - k_s z - \varphi_0)], \tag{1}$$

and

$$E_{pump} = A_{0,p} exp[i(\omega_p t - k_p z - \varphi_0)] \tag{2}$$

where $\omega_{s(p)}$ are the angular frequencies,$k_{s(p)} = 2\pi/\lambda_{s(p)}$ are the wave numbers, $\lambda_{s(p)}$ are the wavelengths and c is the light velocity, z is the position in propagation direction and φ_0 is the initial phase. The configuration shown in Fig. 1, the control intensityI_c inside NFPI [25] consists of output signal intensity (the reflected part) I_{out} and the pump intensity I_p, that means:

$$I_c = I_{out} + I_p, \tag{3}$$

where

$$I_{out} = (1/2)c\,|A_{0,s}|^2\,(1-R) \text{ and } I_p = (1/2)c\,|A_{0,p}|^2, \tag{4}$$

Considering the input angle of both beams $\gamma = 0$, as shown in Ref. [26] and Ref. [25] the path difference of two neighbor rays inside NFPI is given as:

$$\Delta s = 2dn, \tag{5}$$

where

$$n = n_0 + n_2 I_c = n_0 + n_2(|A_{0,s}|^2\,(1-R) + |A_{0,p}|^2), \tag{6}$$

is the refractive index of NM, n_0 is the linear index of NM.

Using Eqs. (5) and (6) we have the phase shift of two neighbor rays inside NFPI given as follows [25, 27]:

$$\begin{aligned} \theta &= \frac{4\pi n_2 d\left[|A_{0,s}|^2\,(1-R) + |A_{0,p}|^2\right]}{\lambda_s} + 2\delta, \\ 2\delta &\approx \frac{4\pi n_0 d}{\lambda_s} + \Delta\varphi, \end{aligned} \tag{7}$$

where $\Delta\varphi$ is the phase shift by the initial refraction of signal light. By the ways as shown in Ref. [25] we have the input-output relation of signal intensities given as follows:

$$I_{out}\left\{1 + \frac{4\mathrm{R}}{(1-R)^2} \times sin^2\phi\right\} = I_{in}, \tag{8}$$

where

$$\phi = \frac{2\pi n_2 d}{\lambda\,(1-R)}\left[(1+R)\,I_{out} + I_p\right], \tag{9}$$

with considering the absorption of NM is negligible. The Eq. (8) describes the input-output relation of signal intensities I_{in} and I_{out} with presence of pump intensity I_p. Here, the pump intensity can be considered as the modulation one influencing on the shape of input-output relation curve, i.e. the stable output intensity can be modulated by the pump intensity. Because the phase shift ϕ nonlinearly depends on the pump intensity, the output signal intensity in the stable region is possible to jump to different values by pump intensity change at certain input signal intensity. It is clear that the Eqs. (8) and (9) describe the input-output relation of signal intensities propagating through NPFI in 1D, at an ideal point, only, so the question is what will this relation occur when use the laser beam with spatial Gaussian distribution?

The intensity distribution sare given as follows:

$$I_{in}(x,y) = I_{0,s}(0,0)exp\left(-2\frac{x^2+y^2}{W_0^2}\right), \tag{10}$$

$$I_p(x,y) = I_{0,p}(0,0)exp\left(-2\frac{x^2+y^2}{W_0^2}\right), \tag{11}$$

where W_0 is the radius of beam waist, $I_{0,s(p)}$ is the peak intensity at spatial position $(x=0, y=0)$.

Substituting Eqs. (10), (11) into Eqs. (8), (9), we have:

$$I_{out}(x,y)\left\{1+\frac{4\mathrm{R}}{(1-R)^2}\times sin^2\phi(x,y)\right\} = I_{in}(x,y), \tag{12}$$

and

$$\phi(x,y) = \frac{2\pi n_2 d}{\lambda\,(1-R)}\left[(1+R)\,I_{out}(x,y)+I_p(x,y)\right], \tag{13}$$

From Eq. (12) we have :

$$I_{out}(x,y) = \frac{I_{in}(x,y)}{\left\{1+\frac{4\mathrm{R}}{(1-R)^2}\times sin^2\phi(x,y)\right\}}, \tag{14}$$

describes the spatial intensity distribution of OSB. As the nonlinear dependence of output signal intensity on the pump intensity, the OSB is reshaped to HGB by suitable pump intensities.

III. SIMULATION RESULTS AND DISCUSSION

The parameters used to design DB-NFPI include: Input signal laser beam with wavelength of $\lambda_s = 0.532$ μm and pump laser beam of $\lambda_p = 1.064$ μm ; After propagating through telescope the waist's radius of two beams of $W_0 = 6$ μm, the Rayleigh ranges of $z_{0,s} \approx 212$ μm; and $z_{0,p} \approx 109$ μm; The mirror's reflection coefficient of $R(\lambda_s) = 75\%$; The ISGB's peak intensity of $I_{o,s} = 0.5 \times 10^3$ W/cm^2, and PGB's peak intensity of $I_{o,p} = (0 \div 10) \times 10^5$ W/cm^2. The ORO's nonlinear coefficient of reflective index of $n_2 = (1.0 \div 10) \times 10^{-7}$ cm$^2/W$ by change its concentration and the thickness $d = (0.01 \div 0.02)$ cm [28]. This thickness is smaller than Rayleigh range ($d = 100$ $\mu m < z_{0,p} < z_{0,z} \approx 212$ μm) of both beams, so Eqs. (10) and (11) will be used to describe the intensity distribution of plane waves inside NFPI. The shape of ISGB and PGB is illustrated in Fig. 2.

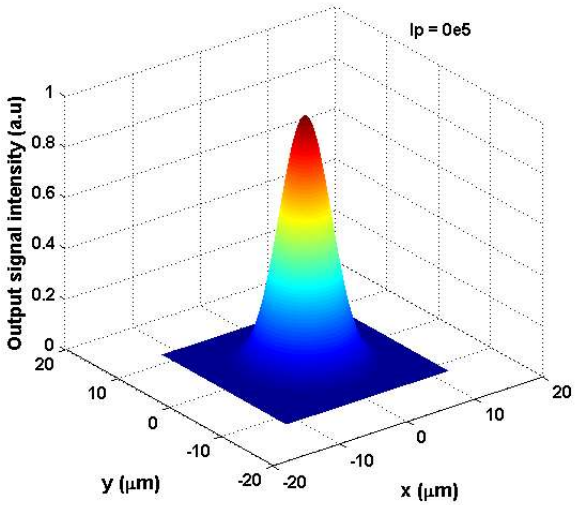

Fig. 2. The intensity spatial distribution of ISGB and PGB.

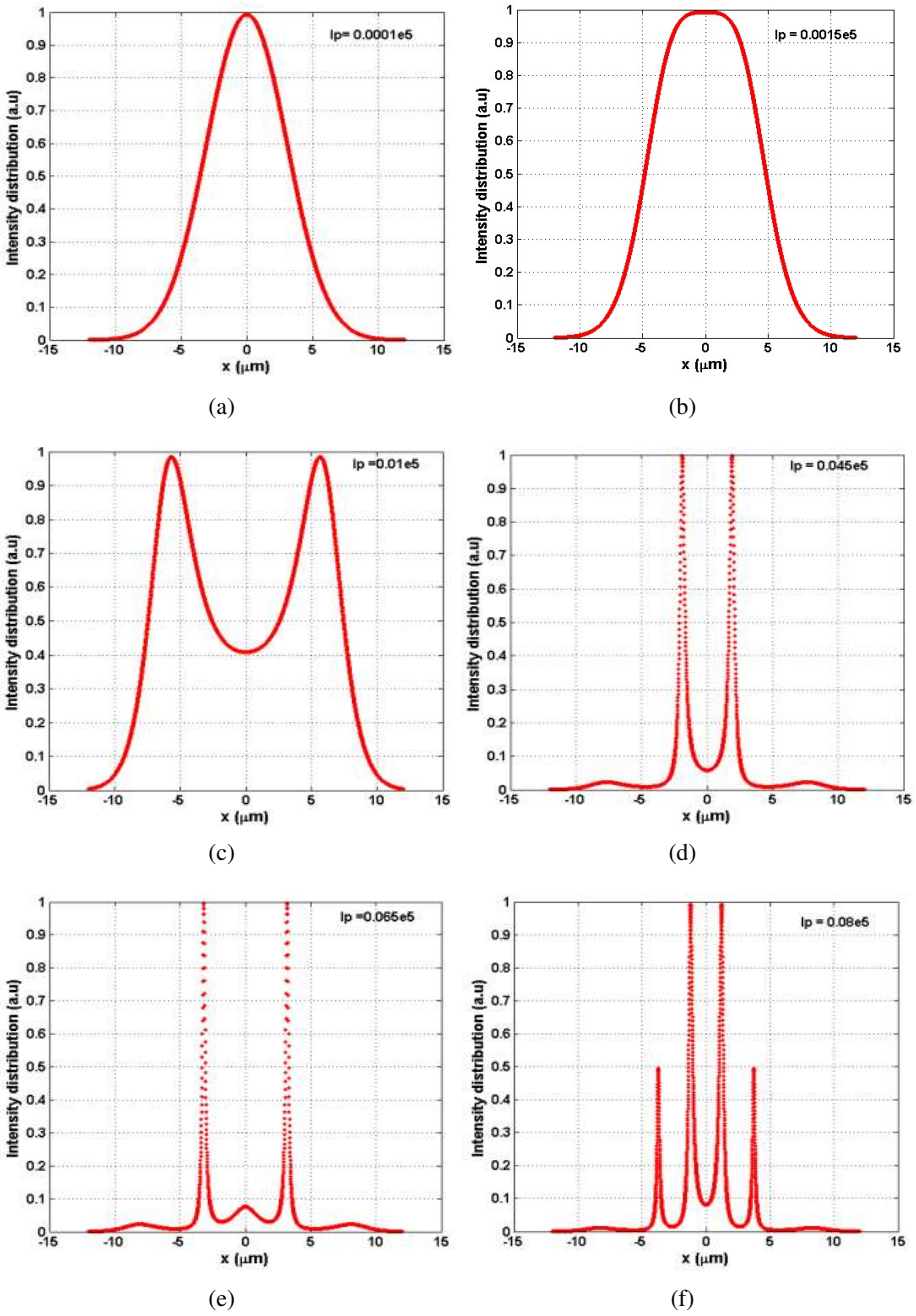

Fig. 3. Intensity 1D distribution of OGB with different pump intensity. $d = 0.018$ cm, $R(\lambda_s) = 75\%$, $I_{o,s} = 0.5 \times 10^3$ W/cm^2, $n_2 = 1.0 \times 10^{-7}$cm^2/W, $W_0 = 6$ μm.

Using Eq. (14), the intensity 1D distribution of OSB is numerically calculated with different pump peak intensities by Matlab software and shown in Fig. 3. The intensity 1D distribution of

OSB is simulated with different peak pump intensities $I_{o,p}$ (or I_p in Fig. 3) of 0.0001×10^5 W/cm^2, 0.0015×10^5 W/cm^2, 0.045×10^5 W/cm^2, 0.06×10^5 W/cm^2 and 0.08×10^5 W/cm^2, other parameters are fixed as above. We see that if the pump peak intensity is smaller than $I_p = 0.015 \times 10^5$ W/cm^2, the OSB remains its Gaussian shape (Fig. 3a), if $I_p = 0.015 \times 10^5$ W/cm^2 it reshaped to the flat-top GB [26] (Fig. 3b), if $I_p = 0.01 \times 10^5$ W/cm^2 toring-GB (Fig. 3c) [29], if 0.045×10^5 W/cm^2 $< I_p < 0.065 \times 10^5$ W/cm^2 to HGB (Fig. 3d, e), and if $I_p > 0.065 \times 10^5$ W/cm^{2}to multi-HGB [30] (Fig.3f). The HG shape of OSB is simulated and shown in Fig. 4.

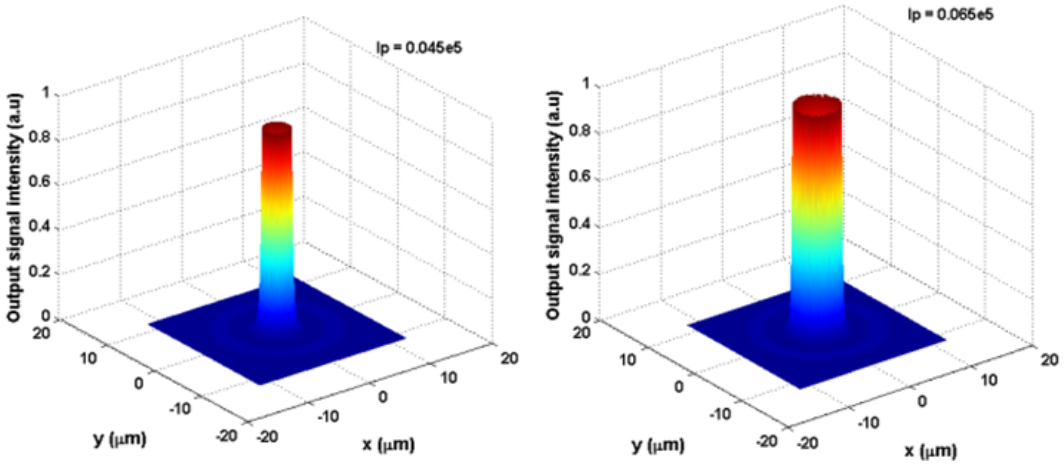

(a) (b)

Fig. 4. HG shape of OSB at $I_{o,p} = 0.045 \times 10^5$ W/cm^2 (a) and $I_{o,p} = 0.065 \times 10^5$ W/cm^2 (b).

For a given collection of design parameters, the OSB is reshaped to HGB if pump peak intensity is in a certain range. This range changes when the one of design parameters changes. The range of pump peak intensity to create HGB for DBNFPI with different nonlinear coefficient of reflective index and thickness of thin film of ORO is presented in Table 1. The obtained results show that the pump peak intensity decreases when nonlinear coefficient of reflective index and thickness of thin film of ORO increases. Thus, use film thicker and organic dye with higher nonlinear coefficient of reflective index, the pump peak intensity will lower. Here, there is an important problem that the pump peak intensity needed to create HGB always is suitable to a collection of other design parameters. This confirms that it is possible to use an added laser GB as the PGB to modulate the OSB of NFPI and the proposed DBFPI like as a device to create the laser HGB for optically microspheres trapping [1, 31].

As shown in Fig.3d,e, the hollow width of HGB is about6μm , approximately equals the ISGB's waist. Comparing the intensity 1D distribution of GB (Fig.3a) and HGB (Fig.3d,e) we can say that the intensity gradient of output HGB is much higher than that of ISGB. Hence, the HGB created by proposed DBNFPI using the pump intensity range given in Table 1 can be used to trap low-index microspheres ($n_{mf}/n_f < 1$) and radius $a < 2.5$ μm [31]. Every principle parts in the proposed model is reachable [14, 17, 25], so the HGB will be set-up and use for optical trap low-index microsphere.

Table 1. The range of pump peak intensity suitable to collection of design parameters of DBNFPI for HGB creation.

α^*	n_2 (10^{-7} cm^2/W)					
	1.0	2.0	4.0	6.0	8.0	10.0
d (mm) 0.10	0.90÷1.10	0.500÷0.550	0.250÷0.280	0.160÷0.190	0.120÷0.140	0.090÷0.110
0.12	0.75÷0.90	0.400÷0.450	0.190÷0.230	0.130÷0.150	0.100÷0.110	0.080÷0.090
0.14	0.65÷0.80	0.350÷0.400	0.250÷0.300	0.120÷0.130	0.080÷0.095	0.065÷0.075
0.18	0.45÷0.65	0.250÷0.300	0.140÷0.150	0.085÷0.100	0.065÷0.075	0.055÷0.060
2.0	0.43÷0.53	0.220÷0.270	0.110÷0.130	0.070÷0.090	0.060÷0.070	0.045÷0.050

* $I_{o,p} = \alpha \times 10^4$ W/cm^2, $W_0 = 6\ \mu$m, $R(\lambda_s) = 75\%$, $I_{o,s} = 0.5 \times 10^3$ W/cm^2

IV. CONCLUSION

The dual-beam nonlinear Fabry-Perot interferometer using two laser GBs, one of them plays the role of signal and another one does that of pump for HGB creation is proposed. The output-input relation of intensities concerning the pump intensityand the expression describing the intensity distribution of OSB are derived. The intensity 1D and 2D distribution of OSB are numerically calculated. The results show that HGB created in the range of pump peak intensity suitable to the collection of designed parameters of DBNFPI. To reduce the pump peak intensity, it is necessary to use thicker film of ORO with higher nonlinear coefficient of reflective index. Using the GBs with waist of 6 μm we can obtain HGB with hollow width 6 μm and very high intensity gradient efficient to optical trap for low-index microspheres. This would be a convenient and powerful way to describe and study the propagation of GB through NFPI, and opens the potential for low-index microspheres trapping and manipulatingby using DBNFPI.

REFERENCES

[1] A. Ashkin, *Biophys. J.* **61** (1992) 569.
[2] S. Pleasants, *Nat. Photonics* **8** (2014) 423.
[3] L. Lu and Z. Wang, *Opt. Commun.* **471** (2020) 125809.
[4] X. Gao, M. Gao, Q. Zhan, J. Li, H. Guo, J. Wang and S. Zhuang, *Optik* **122** (2011) 671.
[5] Y. Nie, X. Li, J. Qi, H. Ma, J. Liao, J. Yang and W. Hu, *Opt. Laser Technol.* **44** (2012) 384.
[6] N. Apurv Chaitanya, A. Chaitanya, J. Banerji and G. Samanta, *Appl. Phys. Lett.* **110** (2017) 211103.
[7] Z. Dai, X. Ling and S. Tang, *Results Phys.* **9** (2018) 215.
[8] G. Zhou, Y. Zhou, Z. Ji and R. Chen, *J. Mod. Opt.* **65** (2018) 2186.
[9] S. Chen, Y. Miao, G. Sui, X. Wu and X. Gao, *Opt. Quantum Electron.* **52** (2020) 22.
[10] L. Zhu, S. Ji, L. Wang, M. Sun, Z. Li, J. Yu and J. Chen, *Axial multifocal spots generated by sectored phase-only modulation under tight focusing condition*, Proceedings Volume 9271, Holography, Diffractive Optics, and Applications VI, vol. 9271, International Society for Optics and Photonics, 2014, p. 92710L.
[11] L. Q. Anh, T. B. Chu and H. Q. Quy, *Comm. in Phys.* **10** (2000) 242.
[12] N. A. Chaitanya, M. Jabir, J. Banerji and G. K. Samanta, *Sci. Rep.* **6** (2016) 32464.
[13] B. E. Saleh and M. C. Teich, *Fundamentals of photonics*, John Wiley & Sons, 2019.
[14] N. Van Hoa, H. Q. Quy and V. N. Sau, *Comm. in Phys.* **21** (2011) 83.
[15] H. Q. Quy, V. N. Sau, N. Van Hoa and N. T. T. Tam, *Comm. in Phys.* **21** (2011) 161.

[16] N. V. Hoa, H. Q. Quy and V. N. Sau, *Close michelson interferometer semi-embedded by nonlinear medium for laser beam redistributing*, Proc. of the Seventh Germane-Vietnam Seminar (GVS7-Halong), vol. 9271, 2005, pp. 166–170.
[17] J. Yuan, W. Feng, P. Li, X. Zhang, Y. Zhang, H. Zheng and Y. Zhang, *Phys. Rev. A* **86** (2012) 063820.
[18] Z. Zhang, H. Chen, L. Zhang, D. Zhang, X. Li, Y. Zhang and Y. Zhang, *EPL (Europhysics Letters)* **117** (2017) 53001.
[19] Z. Zhang, D. Ma, J. Liu, Y. Sun, L. Cheng, G. A. Khan and Y. Zhang, *Opt. Express* **25** (2017) 8916.
[20] D. X. Khoa, P. Van Trong, T. M. Cuong, V. N. Sau, N. H. Bang et al., *Comm. in Phys.* **24** (2014) 217.
[21] H. Hamedi, *Laser Phys.* **27** (2017) 066002.
[22] H. Jafarzadeh, *Laser Phys.* **27** (2017) 025204.
[23] H. M. Dong, L. T. Y. Nga and N. H. Bang, *Appl. Opt.* **58** (2019) 4192.
[24] S. Jeyaram and T. Geethakrishnan, *Opt. Laser Technol.* **89** (2017) 179.
[25] Q. H. Quang, L. M. Van, T. T. Doan, K. B. Xuan, T. N. Manh and Q. H. Dinh, *Appl. Opt.* **59** (2020) 5664.
[26] L. V. Tarasov, *Laser phys.*, MIR, Moscov, 1980.
[27] V. Degiorgio, *Am. J. Phys.* **48** (1980) 81.
[28] L. T. Nguyen, N. T. Hong, C. T. B. Thi and A. Q. Le, *J. Nonlinear Opt. Phys. Mater.* **23** (2014) 1450020.
[29] P. Varshney, A. Upadhayay, K. Madhubabu, V. Sajal and J. Chakera, *Laser Part. Beams* **36** (2018) 236.
[30] A. Endo, K. Karatsu, A. P. Laguna, B. Mirzaei, R. Huiting, D. Thoen, V. Murugesan, S. J. Yates, J. Bueno, N. V. Marrewijk et al., *Journal of Astronomical Telescopes, Instruments, and Systems* **5** (2019) 035004.
[31] Z. Liu, X. Wang and K. Hang, *Sci. Rep.* **9** (2019) 10187.